High Frequency Impedance Measurements for Characterization, Monitoring and Verification Efforts

Ki Ha Lee, Alex Becker, and Louise Pellerin
Lawrence Berkeley National Laboratory
Berkeley, CA 94720

William Frangos, Research Associate

EMSP Project # 60328

Purpose To develop high-frequency impedance methodology for investigation of the near-surface. The specific goal is high-resolution, non-invasive imaging of conductivity and permittivity to depths of a few meters.

Theory

The electromagnetic propagation constant may be resolved into orthogonal components, k_x and k_z

$$k^2 = \varepsilon\mu\omega^2 - i\mu\sigma\omega = k_x^2 + k_z^2$$

Upon oblique incidence at an interface, Snell's Law requires that k_x remain constant, while k_z varies with the properties of the medium. Consequently, propagation below the surface may be in the form of an inhomogeneous wave. This effect becomes particularly important at frequencies between the diffusion and wave propagation regions of the spectrum.

For a homogeneous half-space, the surface impedances for TM and TE modes are, respectively,

$$Z_{TM} = \frac{\mu\omega\cos\theta_1}{k_1} \quad \text{and} \quad Z_{TE} = \frac{\mu\omega}{k_1\cos\theta_1}$$

where è$_1$ is the angle of transmission.

Song, *et al.*, 1996 give the expressions for two layered structures.
The surface impedance observed at oblique incidence may be corrected to that for normal incidence by

$$Z_\perp = \frac{\mu\omega}{k_1} = \frac{\sqrt{2}Z_{TM}}{\left[1+\sqrt{1-\left(\frac{2Z_{TM}k_x}{\mu\omega}\right)^2}\right]^{1/2}} \quad \text{for TM mode, and}$$

$$Z_\perp = \frac{\mu\omega}{k_1} = \frac{\mu\omega}{\sqrt{k_x^2 + \left(\frac{\mu\omega}{Z_{TE}}\right)^2}} \quad \text{for TE mode}$$

Thus, knowledge of k_x is necessary for interpretation.

The horizontal wavenumber, k_x, may be determined by making simultaneous measurements of either the transverse and vertical fields, whereupon

$$k_x = -\varepsilon_0\omega\frac{E_z}{H_y} \quad \text{for TM mode, and}$$

$$k_x = \mu_0\omega\frac{H_z}{E_y} \quad \text{for TE mode,}$$

or the horizontal components at proximate locations, whereupon

$$k_x = \frac{i}{\Delta x}\ln\left(\frac{H_{y1}}{H_{y2}}\right) = \frac{i}{\Delta x}\ln\left(\frac{E_{x1}}{E_{x2}}\right) \quad \text{for TM mode, and}$$

$$k_x = -\frac{i}{\Delta x}\ln\left(\frac{E_{y1}}{E_{y2}}\right) = -\frac{i}{\Delta x}\ln\left(\frac{H_{x1}}{H_{x2}}\right) \quad \text{for TE mode.}$$

The figures at right show k_x determined from numerical model results by both of these methods. The model employs a surface source 100 m away over an earth of 100 Ù-m and å$_r$ = 10.

Horizontal Wavenumber estimated from Numerical Model Results

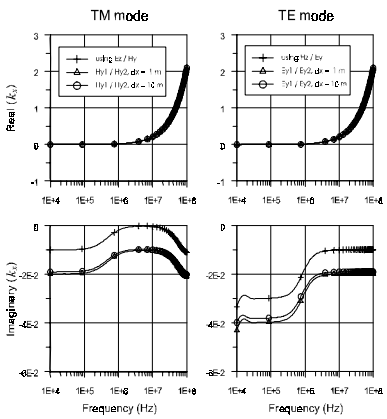

Once the normally-incident surface impedance is known, an apparent resistivity and apparent permittivity may be calculated from

$$Z_\perp^2 = \frac{\mu\omega}{\varepsilon\omega - i\sigma}$$

The figures at the right show apparent resistivity and permittivity for TM and TE modes determined from the model results above.

Apparent Resistivity & Permittivity estimated from Numerical Model

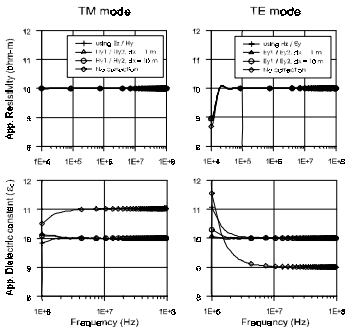

Theory (2)

One-dimensional Inversion

The fields above a two-layer earth can differ markedly from those over a homogenous half space. Of particular note is the resistive-over-conductive case, where reflected waves from the lower interface can interfere with the incident wave at the surface. The figures at the right show the apparent resistivity and apparent permittivity for both TM and TE modes modeled for a three-meter thick upper layer with ñ= 500 Ù-m and å$_r$ = 6 and lower half-space of ñ= 10 Ù-m and å$_r$= 30. The oscillations of the apparent resistivity lead to negative values, indicated by the shading. The various curves are for the different means of estimating the k_x values.

A simulated annealing algorithm (Kim, *et al.*, 1997) has been applied to the model data; results are presented in the lower figure.

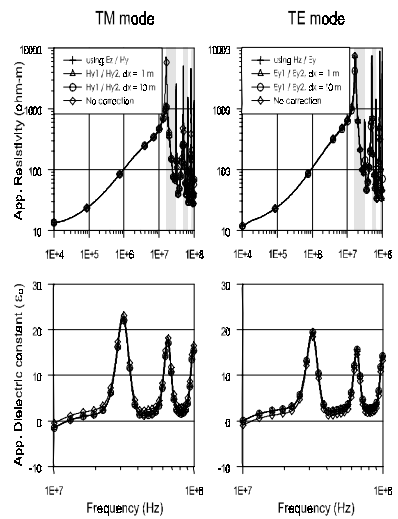

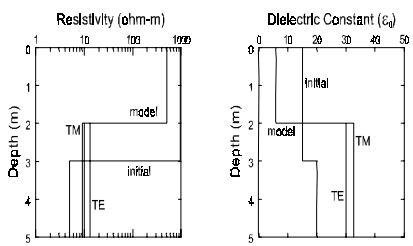

Height-sensitivity Effects

The vector potential due to a short, vertical current element is

$$A(x,y,z)=\frac{\mu}{4\pi}\int_C I_e\frac{e^{-jkR}}{R}dl=\hat{z}\frac{\mu I_0}{4\pi r}e^{-jkr}\int_{-l/2}^{l/2}dz=\hat{z}\frac{\mu I_0 l}{4\pi r}e^{-jkr}$$

which leads to the radiated electric fields

$$E_r=\eta\frac{I_0 l\cos\theta}{2\pi r^2}e^{-jkr}\left[1+\frac{1}{jkr}\right]$$

$$E_\theta=j\eta\frac{kI_0 l\sin\theta}{4\pi r}e^{-jkr}\left[1+\frac{1}{jkr}-\frac{1}{(kr)^2}\right]$$

A vertical stub dipole radiating near the surface of the earth creates a direct and a reflected (image) field at a distant observation point. The sum of these fields may be written as

$$E_\theta\equiv j\eta\frac{kI_0 l\,e^{-jkr}}{4\pi r}\sin\theta\left[e^{jkh\cos\theta}+R_i e^{-jkh\cos\theta}\right]$$

The field due to a stub dipole is thus seen to depend on the angle from the dipole, the height of the antenna above the earth, and the electrical properties of the earth. The top figure shows the vertical-plane radiation pattern rosettes for an infinitesimal dipole at various heights above a ground.

The radiation pattern may also be seen as a sensitivity pattern for a dipole operating as a receiver by judicious application of the Reciprocity Theorem (Rayleigh, 1877, Monteath, 1973). The lower figure presents the relative sensitivity expected for a vertical stub dipole as a function of height above the ground.

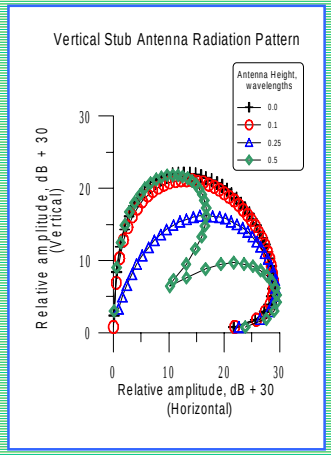

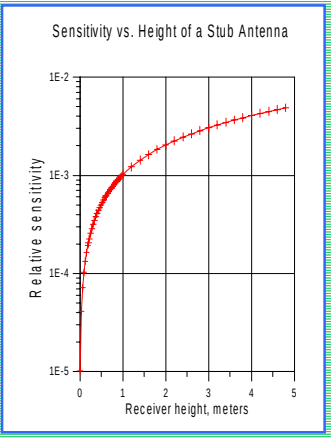

Toroid Electric Sensor

An electric field antenna may be devised that senses components of the magnetic field and takes the vector curl of them (Wait, 1995, Lee, 1997).

$$\nabla \times \vec{H} = (\sigma + i\varepsilon\omega)\vec{E} \quad \text{or,} \quad \vec{E} = \frac{\nabla \times \vec{H}}{(\sigma + i\varepsilon\omega)}$$

The figure at the right illustrates the geometry necessary.

A continuously wound toroidal coil is sensitive to an electric field along its axis, with an antenna factor of

$$AF = V_{out} / E_{incident} = NAD\,k^2$$

where

N = number of turns,
A = Area of coil,
D = Diameter of toroid, and
k = propagation const.

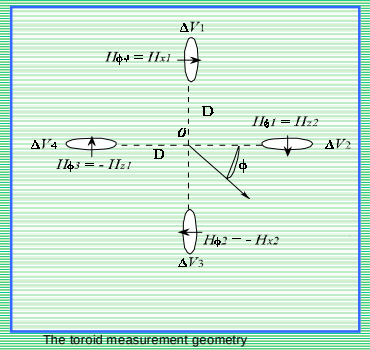

The toroid measurement geometry

Features:

- ✔ Small size
- ✔ Sensitivity increases with square of frequency
- ✔ Small Antenna Factor, Low source impedance
- ✔

A prototype toroid antenna has been built and tested (see figures to the right). The effective source inductance is about 44 ì H, with an effective capacitance of 110 pF. The resulting self-resonance is a major factor in the response.

Electrostatic shielding is important in the design. Two levels of shielding have been implemented to date. Stray pickup still dominates the test results at low frequencies.

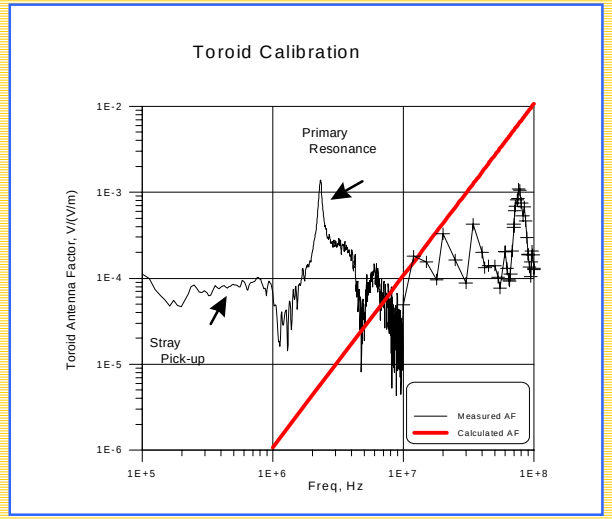

Magnetic Loop Sensor

EMCO Model 6507 Magnetic Field Antenna

- ✔ 1 kHz to 30 MHz response
- ✔ Manufacturer's calibration verified to within 3%
- ✔ Directional sensitivity is typical dipole pattern

Magnetic loop antenna.
Loop diameter is 30 cm.

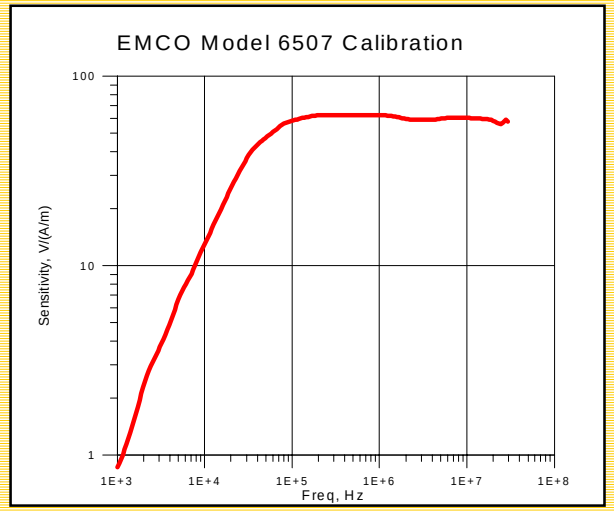

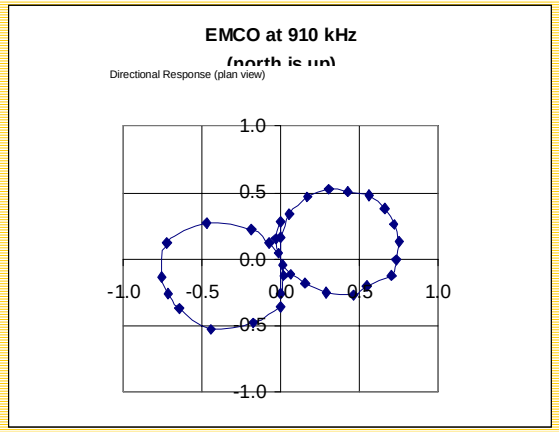

Capacitively-Grounded Dipole

A pair of insulated metallic electrodes placed on the surface of the earth can serve as an electric dipole sensor.

E = V/d

where V is the observed voltage between the plates,
d is the distance between the plates

The source impedance is typically high, requiring special efforts to avoid loading.

Shown at right are results obtained with a 4-m capacitively-coupled dipole and the magnetic loop sensor using

$$\rho_a = \frac{1}{\mu\omega}\left(\frac{E_x}{H_y}\right)^2$$

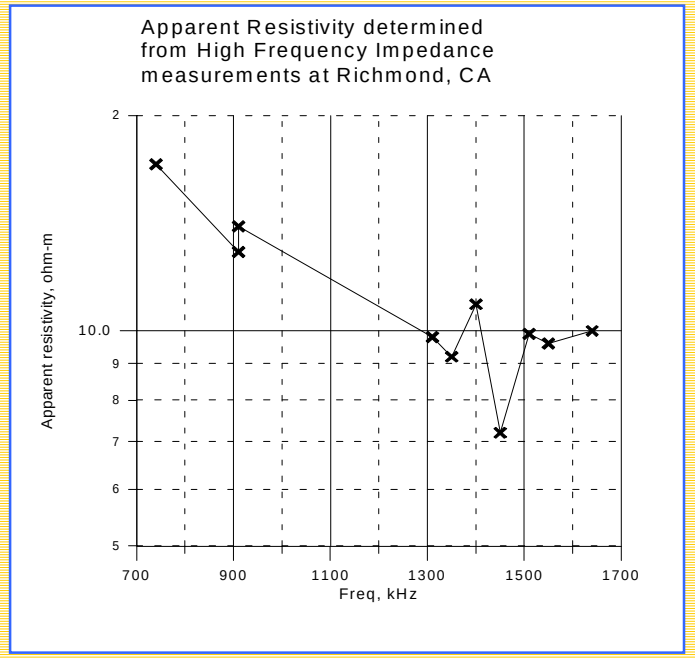

Galvanically determined resistivity:

rho1 = 42 ohm-m, h= 0.46 m
rho2 = 9.6 " " h= 1.95 "
rho3 = 16 " "

Stub Antenna Electric Sensor

ARA Model ADA-120/A Standard E-field Antenna

- ✔
- ✔ 1 kHz to 200 MHz useful frequency range
- ✔
- ✔ Large Antenna Factor, High source impedance
- ✔
- ✔ Sensitivity Pattern varies with height above ground
- ✔
- ✔ Better than 20 dB rejection of orthogonal horizontal component

The response of a short electric dipole with a capacitive load is given by (Kanda, 1994)

$$AF = \frac{V_{Load}}{E_{incid}} = \frac{h\alpha/2}{1 + C/C_a}$$

where $C_a = \frac{4\pi h}{\eta_0 c(\Omega - 2 - \ln 4)}$ is the antenna capacitance

and $\alpha = \frac{\Omega - 1}{\Omega - 2 + \ln 4}$, $\Omega = 2\ln 2h/a$

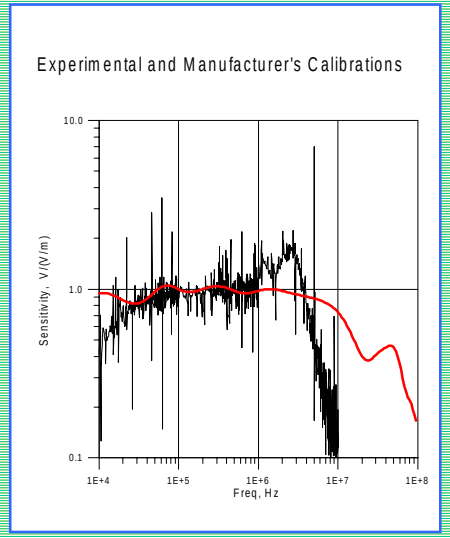

The stub dipole, shown in horizontal mode. Distance between the end plates is 66 centimeters (26 inches).

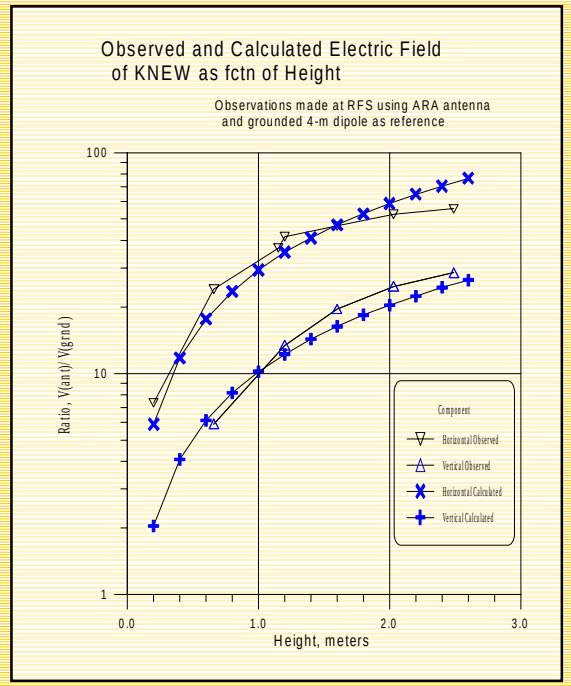

Summary

- ✔ Appropriate theory has been developed for the interpretation of one-dimensional conductivity and permittivity structures.
- ✔ An inversion method has been devised for one-dimensional interpretation.
- ✔ Three electric field sensors are being evaluated:
  - * A prototype toroid antenna has been built and shows promise.
  - * An electrically short stub antenna has been investigated.
  - * The capacitively-coupled grounded dipole antenna yields good results at low end of the spectrum of interest.
- ✔ A magnetic loop antenna has been verified through the midrange of the target spectrum.

Future Work

- ✔ Investigate interpretation techniques for two and three dimensions.
- ✔ Improve the shielding and diminish the self-resonant properties of the toroid antenna.
- ✔ Further resolve the stub antenna height-response function.
- ✔ Extend the magnetic loop antenna response to higher frequencies.

References

Kanda, M., 1994, Standard antennas for electromagnetic interference measurements and methods to calibrate them; IEEE Trans. EM. Compat., vol. 36, no. 4, pp. 261-273

Kim, H.J., Song, Y., and Lee, K.H., 1997, High-frequency electromagnetic inversion for a dispersive layered earth; J. Geomag. Geoelectr., vol. 49, pp. 1439-1450

Lee, K.H., 1997, High-frequency electric field measurement using a toroidal antenna; Lawrence Berkeley National Lab report LBNL-39894, UC-2040

Monteath, G.D., 1973, Applications of the electromagnetic reciprocity principle; Pergamon, Oxford

Rayleigh, J.W.S., 1877, The theory of sound; MacMillan, London

Song, Y., Morrison, H.F., and Lee, K.H., 1996, High frequency electromagnetic impedance for subsurface imaging; SAGEEP '96 (Reno)

Song, Y., Kim, H.J., Morrison, H.F., and Lee, K.H., 1998, High frequency EM impedance method for subsurface imaging; *in press*

Wait, J.R., 1995, Excitation of a conducting half-space by a toroidal coil; IEEE Ant. Prop. Mag., vol. 37, no. 4, pp. 72-74